Journal of Poultry Sciences and Avian Diseases

Journal homepage: www.jpsad.com

Digital Radiography and CT-Scan Findings in Femoral Bone Structures of Long-legged Buzzard (Buteo rufinus)

Basir Abolghasemi[1], Mohammad Reza Esmailinejad[1*], Hemad Shafiei[1], Mohammadjavad Jahedi[1], Nafiseh Alinejad[2]

[1] Department of Clinical Science, Faculty of Veterinary Medicine, Shahid Bahonar University of Kerman, Kerman, Iran
[2] Faculty of Veterinary Medicine, Science and Research Branch, Islamic Azad University, Tehran, Iran

*** Corresponding author email address**: esmaili.mreza@uk.ac.ir

A r t i c l e I n f o

Article type:
Original Research

How to cite this article:
Abolghasemi, B., Esmailinejad, M., Shafiei, H., Jahedi, M., & Alinejad, N. (2026). Digital Radiography and CT-Scan Findings in Femoral Bone Structures of Long-legged Buzzard (Buteo rufinus). *Journal of Poultry Sciences and Avian Diseases, 4*(1), 1-9.
http://dx.doi.org/10.61838/kman.jpsad.158

A B S T R A C T

Veterinary diagnostic methods are rapidly evolving, with radiology techniques playing a key role in clinical activities and disease diagnosis. Computed Tomography (CT) has gained popularity due to its detailed structural imaging capabilities and ability to provide precise diagnostic information. The *Buteo rufinus*, a common bird of prey species admitted to the Environmental Protection Department of Kerman, often presents with skeletal injuries, making advanced imaging techniques valuable for effective treatment. This study examined the femoral bone structure using digital radiology and CT in 10 adult *Buteo Rufinus*. Sedated birds underwent imaging of left and right femur structures, and multiple indices were measured. A significant difference was found in the diameter of the medullary cavity and thickness of the cortex between radiology and CT techniques ($p<0.05$), while no significant difference was observed between left and right femoral indices using either method ($p>0.05$). CT offers higher accuracy in measuring some femur indices and provides precise information for managing femoral injuries in Buteo rufinus. It is recommended for enhancing clinical outcomes in these raptors.

Keywords: *Long-legged buzzard, Femur, Digital radiology, CT-scan, Buteo rufinus.*

1 Introduction

The Long-legged Buzzard (*Buteo rufinus*) is a large raptor, 50-65 cm in length with a 126-148 cm wingspan. It resembles the Common Buzzard but has longer wings and tail, and its plumage varies from brownish-red to blackish-brown. Adults typically have brown upperparts, a light rufous head, and a darker rufous-brown belly, while juveniles are paler with a lighter tail and distinct stripes.

Article history:
Received 07 September 2025
Revised 20 September 2025
Accepted 13 October 2025
Published online 01 January 2026

It inhabits arid or semi-arid regions, such as steppes, deserts, and mountains. It is a solitary or paired bird, often seen perched or hovering while hunting small mammals, reptiles, and large insects. Breeding occurs from March to April, with 2-3 eggs per clutch.

The species is commonly found in Iran's steppes, hills, and mountains, and in winter, it moves to the southern regions. It is protected in Iran due to its conservation value (1).

Wild birds of prey, especially raptors, are often presented for skeletal injuries. Trauma is particularly common among Falconiformes, finally resulting in euthanasia or spontaneous death (2, 3).

Therefore, identifying bone structures using diagnostic imaging as a non-invasive method in birds of prey is particularly important for the examination, treatment, and rehabilitation process of these birds (4).

Many bones, including some cervical vertebrae, humerus, femur, and sternum, are pneumatized. This process involves filling these bones with air, a characteristic feature of species with an advanced respiratory system, such as birds. Notably, some of these pneumatized bones, such as the humerus, are directly connected to the respiratory system through air sacs. This anatomical adaptation has significant clinical implications, especially when treating fractures. The close association between these bones and the respiratory system necessitates careful consideration in medical interventions to avoid potential complications related to respiratory function during fracture management (5).

While pneumatization provides advantages, it also makes bones more brittle. They are prone to shattering or fragmenting upon impact, and their distal extremities have limited soft tissue support. This increases the risk of open, comminuted fractures and complications during repair (6).

In birds, fractures of pneumatic bones, such as the femur, can lead to respiratory infections, especially in cases of open fractures (6).

Similar to mammals, the femur connects proximally with the pelvis at the coxofemoral joint. This connection is reinforced by a robust ligament that attaches the head of the femur, bridging the short distance between the acetabulum and the fovea capitis on the femoral head (7).

The broader availability of modern and non-invasive imaging modalities, including digital radiography and CT-Scan, has significantly enhanced diagnostic accuracy in the field of wild and exotic animal medicine (4, 8).

Radiographs are highly valuable for assessing the musculoskeletal system, helping to identify the cause of lameness and evaluate the extent of bone involvement and soft tissue injuries. The fundamental principles of radiographic interpretation used in mammals also apply to birds when examining their musculoskeletal system (9). Although conventional radiography is widely employed in veterinary practice for visualizing both soft and hard tissues, it is constrained by the superimposition of anatomical structures. Conversely, computed tomography (CT) enables the simultaneous visualization of tissues without overlapping, providing high-definition images and accurately evaluating representations of pathological alterations (10, 11).

In this context, there is an increasing need for a thorough understanding of normal anatomy in healthy animals through the use of diagnostic imaging. This knowledge would enhance the ability to accurately identify and interpret pathological conditions in the Long-legged Buzzard.

2 Materials and Methods:

Animals: In Kerman province, a protected wildlife rehabilitation center receives injured birds referred by environmental guards for treatment. Ten mature Long-legged buzzards (Buteo rufinus), each weighing between 650 and 750 grams, were selected for this study.

In this study, the sex and precise age of Long-legged Buzzards (Buteo rufinus) could not be determined. The species' monomorphic nature prevents sex identification based on external morphology. Conducted outside the breeding season, the study lacked observable reproductive behaviors, and radiographic imaging showed no active gonads. Regarding age, all birds were examined by an avian specialist and confirmed to be mature based on physical characteristics. However, due to the absence of reliable indicators for precise age determination, only their maturity could be noted, and their exact age remained undetermined.

All birds were wild animals under medical care at the Kerman Rehabilitation Center, referred by the Environmental Protection Department of Kerman. Prior to the study, the birds underwent physical examinations to ensure they were free from any health complications that could potentially influence the results. Subsequently, the birds were sedated with a combination of ketamine (20 mg/kg) and diazepam (1 mg/kg) administered intramuscularly to minimize stress and movement during the imaging procedures. Following sedation, digital radiography and computed tomography (CT) imaging were performed on the whole body, followed by specific analysis of the wings.

Diagnostic Imaging Protocol: Two standard orthogonal views were obtained for each leg (medio-lateral and cranio-caudal projections). The bird was positioned in lateral recumbency. The non-dependent limb was extended caudally, while the limb of interest was positioned in a true lateral projection, adjacent to the cassette, and stabilized with tape. And in the other position, birds were placed in dorsal recumbency with their legs extended for proper positioning. Direct Digital Radiography (A fix x-ray generator, GAMI, DR model, Milan, Italy) with parameters set at KVp: 60 and mAs: 2.5 with a source-to-detector distance of 90 cm. All imaging was performed by a single individual (CLM). Images were stored in a picture-archiving and communication system (PACS) for further analysis.

Computed Tomography: All imaging was performed using an 8-slice scanner (NeuViz 16 Essence, a multi-slice ultra-fast CT scanner manufactured by Neusoft, Shenyang, China). The animals were positioned in dorsal recumbency, and their wings and legs were secured using microporous surgical tape to prevent movement during the scans. All scans were performed with settings of 120 kVp and 150 mAs, a rotation time of 1 second, a slice thickness of 1 mm, and a pitch of 1. Following the scans, the images were transmitted to the acquisition workstation and subsequently reconstructed into bone planes using specialized software (PACSPLUS, Medical Standard workstation version 3.0).

Measured Parameters: Eight parameters were assessed in both radiology and CT imaging, as detailed: cranio-caudal diameter of bone (measurement of bone diameter from the cranial cortex to the caudal cortex), diameter of the medullary cavity (measurement of the internal diameter of the bone's medullary cavity at specific sections), thickness of the cortex (evaluation of the cortical bone's thickness) (Figure 1 and Figure 2), proximal to distal length (measurement of the total length of the femur from the proximal to the distal end), thickness of soft tissue (evaluation of the soft tissue in the middle region) (Figure 3), and bone density (analysis of bone opacity using pixel value and Hounsfield unit at the cortex, medullary cavity, and surrounding soft tissue). These parameters were meticulously measured and recorded for comparative analysis between the two imaging modalities to evaluate their diagnostic accuracy and clinical utility.

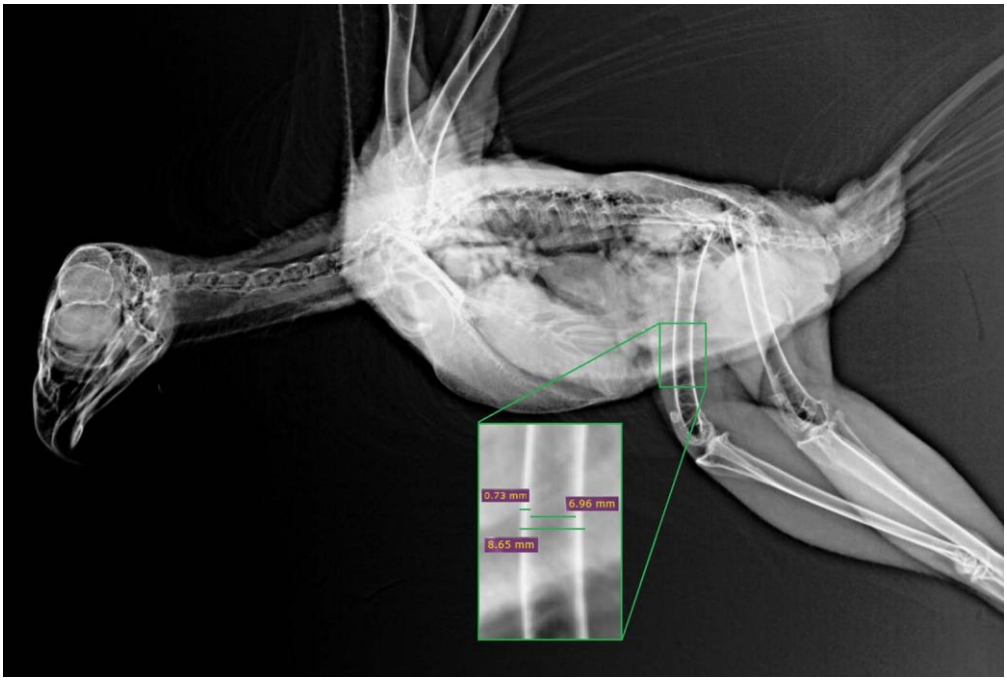

Figure 1. Medio-lateral radiograph of the right leg of Long-legged Buzzard, showing the bone diameter, cortical thickness, and medullary cavity thickness

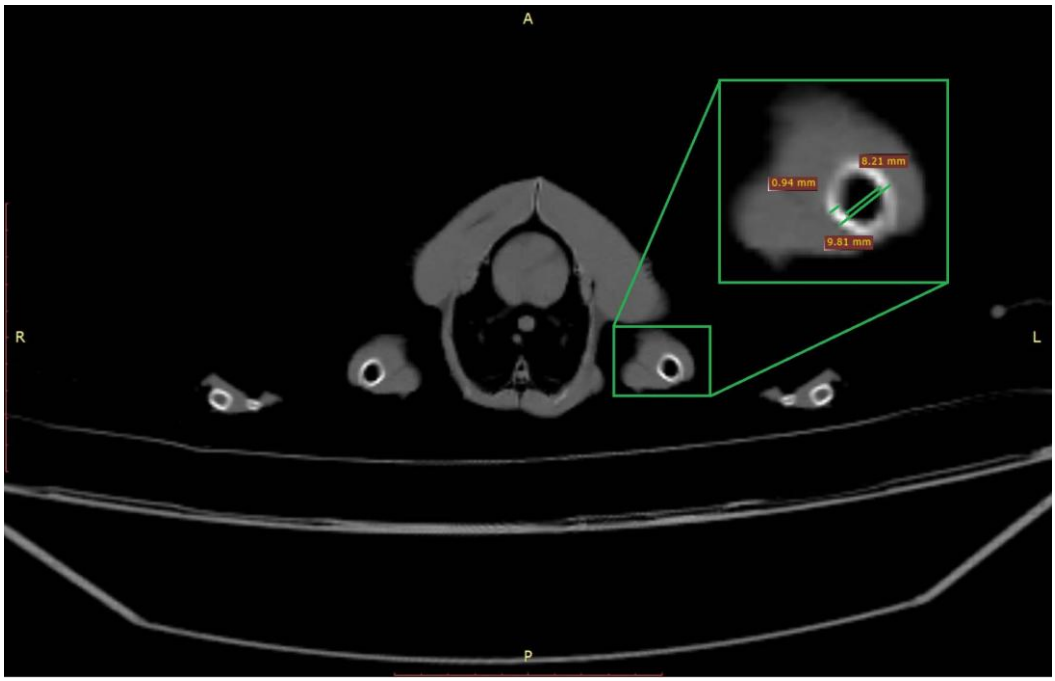

Figure 2. Transverse plane CT scan of the coelomic cavity and both legs of Long-legged Buzzard, showing measurements of bone diameter, cortical thickness, and medullary cavity thickness.

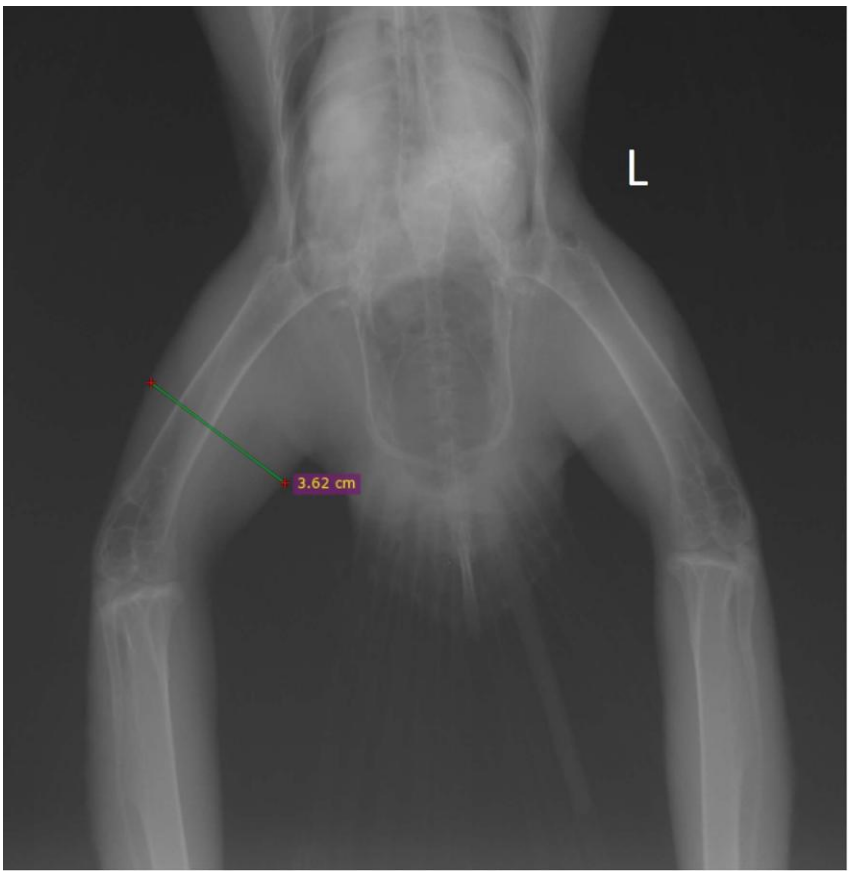

Figure 3. Ventro-dorsal radiograph of the pelvic and legs of Long-legged Buzzard showing the thickness of soft tissue in the middle part of the right femur.

Statistical Analysis: All data collected in this study were analyzed using SPSS statistical software version 21, and results were presented as Mean±Standard Deviation (SD). For this analysis, t-tests and paired t-tests were employed. A significance level of 0.05 was established for this study.

3 Results

Table 1 presents the results of femoral bone parameter measurements obtained from digital radiography, while Table 2 displays the same parameters measured via CT scan for comparative purposes between the left and right legs.

Table 1. Examination of Descriptive Statistics in Radiology Technique for Right and Left Wings

Variable (mm)	Minimum		Maximum		SD		Mean		*p*-value
	Right	Left	Right	Left	Right	Left	Right	Left	
Cranio-caudal diameter of bone (mm)	7.870	7.810	10.03	10.04	0.7042	0.6980	8.744	8.811	0.8608
Diameter of medullary cavity (mm)	6.430	6.530	8.920	8.940	0.8222	0.7791	7.211	7.427	0.8608
Thickness of cortex (mm)	0.7400	0.6600	0.9600	0.9800	0.08050	0.1184	0.8514	0.7829	0.2292
Proximal to distal length (mm)	84.20	85.10	100.8	98.80	5.168	4.566	90.63	91.07	0.8675
Thickness of soft tissue in middle part (mm)	32.40	30.04	42.60	42.70	3.500	3.796	36.10	35.43	0.7389
Cortex value (pixel value)	6046	6450	7034	7431	347.2	333.8	6639	6742	0.5825
Medullary cavity value (pixel value)	5100	5325	8210	8411	1140	1099	7376	7500	0.8397
Soft tissue value (pixel value)	5340	4959	9100	8720	1356	1397	7491	7612	0.8721

Table 2. Measurement of Humeral Indices in the CT-Scan Method

Variable	Minimum		Maximum		SD		Mean		*p*-value
	Right	Left	Right	Left	Right	Left	Right	Left	
Cranio-caudal diameter of bone (mm)	9.530	7.500	10.07	10.07	0,1991	0.9591	9.860	9.674	0.6245
Diameter of medullary cavity (mm)	7.000	6.400	8.710	9.140	0.6078	0.8959	8.050	8.280	0.5844
Thickness of cortex (mm)	0.7600	0.8300	1.030	1.080	0.09394	0.08118	0.8929	0.9329	0.4107
Proximal to distal length (mm)	84.70	85.20	97.40	97.25	4.385	4.428	88.93	89.74	0.7378
Thickness of soft tissue in middle part (mm)	30.50	27.80	35.00	33.90	1.560	2.089	32.07	31.66	0.6806
Cortex value (HU)	295.0	344.0	780.0	860.0	163.5	187.0	416.3	439.0	0.8129
Medullary cavity value (HU)	-970.0	-953.0	-850.0	-800.0	39.99	64.62	-913.9	-888.0	0.3857
Soft tissue value (HU)	53.00	52.00	79.00	77.00	9.144	8.976	62.57	62.29	0.9539

The comparison between digital radiography and CT scan imaging revealed significant differences in their effectiveness for assessing the femur in Buteo rufinus (Table 3). Although radiography provided an overall view of the bone structure, the CT scan provided more precise measurements of internal features, such as the thickness of the cortex and the diameter of the medullary cavity. However, no statistically significant difference was found in the cranio-caudal diameter of the bone between digital radiography and CT scan techniques (p>0.05). Nonetheless,

the CT scan consistently provided more precise measurements than radiography and demonstrated superiority in distinguishing between the cortex and medullary cavity, with significant statistical differences (p<0.05).

Table 3. Comparison of Mean Humerus Features in CT-Scan and Radiology for Right and Left Wings

	Paired Differences							
				95% Confidence Interval of the Difference				
	Mean	Std. Deviation	Std. Error Mean	Lower	Upper	t	df	Sig. (2-tailed)
cranio-caudal diameter of bone CT-radiology	-.41214	91258	24390	-93905	11477	-1.690	13	.115
diameter of the medullary cavity CT-radiology	-.68071	88995	23785	-1.19455	-.16687	-2.862	13	.013
thickness of the cortex CT-radiology	-.09571	12847	03433	16989	-.02154	-2.788	13	.015
proximal to distal length CT-radiology	1.87571	3.41652	91310	-09693	3.84836	2.054	13	.061
thickness of soft tissue CT-radiology	1.90357	3.54185	94660	-14143	3.94857	2.011	13	.066

The cranio-caudal diameter of the bone, measured using CT scan, was 9.39±0.05 mm, and with digital radiography, it was 8.97±0.05 mm, highlighting a negligible difference between the two measurement methods. Similarly, the diameter of the medullary cavity averaged 8.16±0.05 mm with the CT scan and 7.48±0.05 mm with digital radiography, demonstrating that the CT scan provided a more distinct view of the medullary cavity. In terms of cortex analysis, the CT scan reliably visualized the cortical thickness, which averaged 0.91±0.05 mm, whereas radiography measured it as 0.81±0.01 mm.

Key measurements of the femoral structure were consistent across specimens. The average proximal-to-distal length was measured as follows: digital radiography, 90.99±0.05 mm; CT scan, 89.11±0.05 mm, with no significant variation between the left and right sides in each technique (p>0.05).

Measurements of soft tissue thickness in the midsection. The mean thicknesses were as follows: midsection, 34.76±0.05 mm for digital radiography and 32.86±0.05 mm for CT scan.

The analysis of pixel values in the cortex (6690), medullary cavity (7438), and surrounding soft tissues (7551) demonstrated comparable results. Similarly, the evaluation of Hounsfield units (HU) in the cortex (427), medullary cavity (900), and surrounding soft tissues (62) revealed no notable variation between the right and left wings. The Hounsfield unit (HU) of 800±50 indicated density variations reflecting the degree of pneumatization.

4 Discussion

Understanding the Structural features of avian long bones, particularly in raptors, is crucial for accurate diagnosis, surgical planning, and the development of specific rehabilitation protocols. The present study focused on comparing digital radiography and computed tomography (CT) in the evaluation of the femoral bone in the Long-legged Buzzard (Buteo rufinus), using eight distinct morphometric parameters. Among these, statistically significant differences were observed only in the cortical and medullary diameters, suggesting that CT imaging offers superior resolution and reliability in visualizing internal osseous structures compared to conventional radiographic techniques (12).

In the context of avian diagnostic imaging, conventional radiography has long served as the frontline modality due to its availability, low cost, and rapid execution. However, its limitations include the superimposition of structures, poor depth resolution, and low sensitivity in detecting subtle internal variations, which have been well-documented. This is particularly critical in birds, whose bones are often thin-walled, pneumatic, and complex in morphology. CT, by offering high-resolution three-dimensional reconstructions, provides a non-destructive yet highly detailed alternative that facilitates precise assessment of both cortical and trabecular bone components.

Although anatomical dissection remains the gold standard for in-depth analysis of skeletal structures, it is inherently invasive, requires cadaveric material, and is therefore unsuitable for clinical or longitudinal investigations. The inability to apply dissection-based approaches in living specimens highlights the value of imaging modalities, such as CT and radiography, especially in wild or endangered birds, where conservation ethics limit the use of destructive methods. In the current study, the use of CT and radiography allowed for non-invasive evaluation of critical morphometric features without compromising the integrity of the birds (13).

The femur, a load-bearing bone in birds of prey, plays a pivotal role in terrestrial locomotion, take-off propulsion, and prey manipulation. Given its functional importance, a detailed evaluation of its structure is essential, especially in cases of trauma or congenital deformities. Parameters such as cortical thickness and medullary canal diameter are key indicators of biomechanical integrity and load-bearing capacity (14). Our findings suggest that CT images facilitate more accurate quantification of these parameters, which can have direct implications for selecting implant types, assessing fracture severity, and evaluating healing progression.

These results are in line with previous reports emphasizing the diagnostic superiority of CT. Bertuccelli et al. (2021) demonstrated, in their comparative study of humeral bones across raptor species, that CT provides critical insights into species-specific structural adaptations, particularly variations in trabecular density and cortical thickness. While their study focused on the humerus, the methodological implications are equally applicable to femoral analysis, especially considering the mechanical load borne by the femur during flight take-off and land-based movement (15).

Similarly, Souza de Lima et al. (2023) utilized both CT and radiography to generate 3D digital bone models of Rupornis magnirostris, a neotropical raptor, thereby enabling enhanced visualization of complex anatomical features. These digital reconstructions not only supported clinical diagnostics but also proved invaluable in preoperative planning, particularly in determining the geometry and placement of surgical implants. The present study parallels these findings by confirming the capacity of CT to detect internal bone variations that radiography tends to underestimate or overlook (16).

Another significant contribution to the field has been made by Schneider et al. (2024), who utilized micro-CT to examine avian mummified remains. Their work demonstrated the capacity of CT to reveal minute anatomical details in both modern and archaeological specimens, underscoring its versatility and potential for retrospective analyses. While micro-CT may not yet be widely accessible in veterinary clinics, its diagnostic precision sets a benchmark for standard CT modalities used in live birds (17).

Moreover, the biomechanical relevance of internal bone structures, particularly in relation to trabecular-cortical dynamics, has been addressed by Fajardo et al. (2007). They described how, in pneumatic bones common in birds, load-bearing areas often exhibit compensatory densification of trabecular bone despite thinner cortical layers (18). CT scanning, with its high contrast resolution, is uniquely capable of capturing these microstructural adaptations, providing a more comprehensive assessment of bone health and functionality than radiography alone (19).

From a clinical perspective, accurate imaging of the femur is critical in cases involving fractures, metabolic bone disease, neoplasia, or developmental anomalies. The enhanced visualization provided by CT can assist clinicians in classifying fracture types, identifying microfractures or callus formation, and guiding surgical interventions such as pin placement or external fixation. It also enables the measurement of medullary canal diameter—a crucial factor in determining the appropriate size and fit of orthopedic implants.

Furthermore, the importance of imaging precision extends beyond clinical treatment and into avian conservation. Birds of prey are often subject to anthropogenic threats such as collisions, gunshot injuries, and electrocutions, all of which frequently affect the appendicular skeleton (20). CT imaging not only improves individual patient outcomes but also contributes to population-level management strategies by enabling the collection of accurate data on injury prevalence, severity, and response to treatment protocols.

This study has certain limitations that should be acknowledged. First, although the use of a 16-slice or higher CT scanner would provide higher resolution and more accurate measurements, our research team had access only to an 8-slice CT scanner due to equipment availability constraints. Nevertheless, the applied protocol allowed us to obtain diagnostically acceptable images for this study. Second, while a shorter CT gantry rotation time (e.g., 0.5 seconds) could potentially improve image quality and reduce motion artifacts, the scanner available for this study did not

permit rotation times shorter than 1 second. Moreover, reducing the rotation time below this level on the current device would have resulted in a noticeable decrease in image quality due to the scanner's technical characteristics. As a result, the acquisition parameters were optimized within the technical limitations of the device to ensure the best possible image quality.

5 Conclusion

Despite the demonstrated advantages of CT, some limitations persist. High operational costs, limited accessibility in field settings, and the need for general anesthesia during scanning procedures may limit its routine use in wildlife rehabilitation centers. Nonetheless, its application in critical cases, particularly those involving high conservation value species or complex orthopedic injuries, is well justified. As CT technology becomes more portable and cost-effective, its integration into routine avian veterinary practice is expected to expand.

Acknowledgements

The authors gratefully acknowledge the assistance of the Environmental Protection Department of Kerman and the Research Council of Shahid Bahonar University of Kerman for their technical support and knowledge.

Conflict of Interest

The authors declare no competing interests.

Author Contributions

BA: Writing - review & editing, MRE: Conceptualization, Methodology, Data curation, Investigation, Validation, Supervision, Writing - review & editing, HSh: Conceptualization, Investigation, Validation, Supervision, Project administration, Resources, MJ: Formal analysis, Visualization, Writing - original draft, Writing - review & editing, NA: Funding acquisition, Software.

Data Availability Statement

The data that support the findings of this study are available from the corresponding author upon reasonable request.

Ethical Considerations

In conducting this study, all procedures in this study were conducted in accordance with accepted ethical standards for animal research. The protocol was reviewed and approved by the Faculty of Veterinary Medicine, University of Kerman, Iran (Approval Code: 95469605-1404). Radiography and CT-scan examinations were performed by qualified personnel using appropriate handling procedures to minimize stress and ensure animal welfare.

Funding

No funding was received for this research.

References

1. Khaleghizadeh A, Mohammad K, Mansour A, Mohammad T, Alireza H, Seyed Babak M, et al. Atlas of Birds of Iran: Iran Department of the Environment, Tehran; 2020. 617-103 p.
2. Forbes NA. Avian orthopedics. Veterinary Quarterly. 1998;20(sup1):S69-70. doi: 10.1080/01652176.1998.10807421.
3. Molina-López RA, Casal J, Darwich L. Causes of morbidity in wild raptor populations admitted at a wildlife rehabilitation centre in Spain from 1995-2007: a long term retrospective study. PLoS One. 2011;6(9):e24603. doi: 10.1371/journal.pone.0024603.
4. Silva IA, Vieira LC, Mancini VRM, Faillace ACL, Santana MIS. Radiographic anatomy of the cockatiel (Nymphicus hollandicus) axial and appendicular skeleton. Anat Histol Embryol. 2020;49(2):184-95. doi: 10.1111/ahe.12510.
5. Naguib M. Avian radiography and radiology part 2. Companion Anim. 2017;22(10):614-21. doi: 10.12968/coan.2017.22.10.614.
6. Bennett RA, Kuzma AB. Fracture management in birds. Journal of Zoo and Wildlife Medicine. 1992:5-38.
7. Orsini JA, Grenager NS, de Lahunta A. Comparative Veterinary Anatomy: A Clinical Approach: Academic Press; 2021.
8. Ricciardi M, Franchini D, Valastro C, Ciccarelli S, Caprio F, Eyad Assad A, et al. Multidetector computed tomographic anatomy of the lungs in the loggerhead sea turtle (Caretta caretta). Anat Rec. 2019;302(9):1658-65. doi: 10.1002/ar.24030.
9. Hanna AL, Logsdon ML, Mattoon JS. Radiographic Evaluation of Normal and Common Diseases2021. 173-91 p.
10. Krautwald-Junghanns ME, Kostka VM, Dörsch B. Comparative studies on the diagnostic value of conventional radiography and computed tomography in evaluating the heads of psittacine and raptorial birds. J Avian Med Surg. 1998:149-57.
11. Nejad MRE, Vafaei R, Masoudifard M, Nassiri SM, Salimi A. Aggressive chondroblastic osteosarcoma in a dog: A case report: Faculty of Veterinary Medicine, Urmia University, Urmia, Iran; 2019. 361 p.
12. Delibaş V, Soygüder Z, Göya C, Aslan L, Çakmak G. Three-Dimensional Examination of Humerus and Antebrachium Bones in the Red hawk (Buteo Rufinus) with Computed tomography (CT). Van Veterinary Journal. 2024;35(1):70-6. doi: 10.36483/vanvetj.1396960.
13. Lautenschlager S, Bright JA, Rayfield EJ. Digital dissection-using contrast-enhanced computed tomography

scanning to elucidate hard-and soft-tissue anatomy in the common buzzard Buteo buteo. J Anat. 2014;224(4):412-31. doi: 10.1111/joa.12153.
14. Habib MB, Ruff CB. The effects of locomotion on the structural characteristics of avian limb bones. Zool J Linn Soc. 2008;153(3):601-24. doi: 10.1111/j.1096-3642.2008.00402.x.
15. Bertuccelli T, Crosta L, Costa GL, Schnitzer P, Sawmy S, Spadola F. Predisposing anatomical factors of humeral fractures in birds of prey: a preliminary tomographic comparative study. J Avian Med Surg. 2021;35(2):123-34. doi: 10.1647/19-00006.
16. de Lima LFS, de Barros AJBP, Colodel EM, Nespoli PEB, Gomes LG, de Souza RL. Radiographic, tomography and three-dimensional description of the clinical anatomy of the long bones of Rupornis Magnirostris. OBSERVATÓRIO DE LA ECONOMÍA LATINOAMERICANA. 2023;21(10):16852-73. doi: 10.55905/oelv21n10-126.
17. Scholarship W, Schneider MA. Birds of the ancient Nile: Species identification in Egyptian animal mummies using multi-resolution computed tomography and deep learning image segmentation 2024.
18. Fajardo RJ, Hernandez E, O'Connor PM. Postcranial skeletal pneumaticity: a case study in the use of quantitative microCT to assess vertebral structure in birds. J Anat. 2007;211(1):138-47. doi: 10.1111/j.1469-7580.2007.00749.x.
19. Burghardt AJ, Link TM, Majumdar S. High-resolution computed tomography for clinical imaging of bone microarchitecture. Clin Orthop Relat Res. 2011;469(8):2179-93. doi: 10.1007/s11999-010-1766-x.
20. Orosz S, Echols S, Redig P. Avian Surgical Anatomy and Orthopedic Management: Teton NewMedia; 2023.